Contents lists available at ScienceDirect

Catena

journal homepage: www.elsevier.com

Coastline shift analysis in data deficient regions: Exploiting the high spatio-temporal resolution Sentinel-2 products

A. Saleem *, J.L. Awange

School of Earth and Planetary Sciences, Discipline of Spatial Sciences, Curtin University, Perth, Australia

ARTICLE INFO

Keywords:
Coastal erosion
Somalia
Sentinel-2
Remote sensing
Liberia
Coastal shift

ABSTRACT

In most developing countries, coastline shift monitoring using in-situ (ground-based) data faces challenges due, e.g., to data unreliability, inconsistency, deficiency, inaccessibility or incompleteness. Even where practically applicable, the traditional "boots on the ground" methods are labour intensive and expensive, thus imposing burden on poor countries struggling to meet other urgent pressing daily needs, i.e., food and medicine. Remote sensing (RS) techniques provide a more efficient and effective way of collecting data for coastline shift analysis. However, moderate spatio-temporal resolution RS products such as the widely used Landsat products (30 m and 16 days) may be insufficient where high accuracy is desired. In 2015, Sentinel-2 Multi-Spectral Instrument (MSI) remotely sensed products with higher spatio-temporal resolution (10 m and 5 days) and high spectral resolution (13 bands), which promises to improve coastline movement monitoring to high accuracy, was launched. Using two war-impacted countries (Liberia and Somalia) as case studies of regions with data deficiency or of poor quality, for the period 2015–2018, this contribution aims at (i) assessing the suitability of the new freely available high spatio-temporal Sentinel-2 products to monitor coastline shift, (ii) assessing the possibility of filling the missing Sentinel-2 gaps with Landsat 8 panchromatic band (15 m) products to provide alternative data source for mapping of coastline movements where Sentinel-2 data is unusable, e.g., due to cloud cover, and (iii), undertake a comparative analysis between Sentinel-2 (10 m), Landsat panchromatic (15 m), and Landsat multi-spectral (30 m). The results of the evaluation indicate 23% (on average) improvement gained by using Sentinel-2 compared to the traditional Landsat 30 m resolution data (i.e., 32% for Liberia and 14% for Somalia). A comparison of 100 check points from Google Earth Pro (i.e., surrogate in-situ reference data) show 91% agreement for Liberia and 85% for Somalia, indicating the potential of using Sentinel-2 data for future coastal shift studies, particularly for the data deficient regions. The results of comparative studies for Sentinel-2, Landsat panchromatic (PAN), and Landsat multi-spectral (MS) show that the percentages of Sentinel-2 and Landsat PAN that falls within 10 m threshold is much higher than Landsat MS by 35% and 26%, respectively, and for the 2016–2017 period, they provide more detailed mapping of the Liberian coastline compared to Landsat MS (30 m). Finally, panchromatic Landsat data with 15 m resolution are found to be capable of filling the missing Sentinel-2 gaps, i.e., where cloud cover hampers its usability.

1. Introduction

Coastline, the border between water and land is one of the Earth's most dynamic features (Alesheikh et al., 2007). With approximately 60% of the world's population living along the coastal regions, and almost 25% of production taking place within it (Appeaning Addo et al., 2008; Tochamnanvita and Muttitanon, 2014), its constant monitoring is vital given its importance as an ecosystem for economic, ecological, political and social activities. Constant monitoring of coastlines is thus paramount for a sustainable use of its resources. The importance of coastline monitoring is highlighted, e.g., by Li et al. (1998), Di et al. (2003), Veloso-Gomes et al. (2008), Awange et al. (2018) and Gonçalves and Awange (2017) who opine that coastline mapping is critical for safe navigation, coastal resource management, coastal environmental protection, integrated coastal zone management (ICZM, i.e., management of coastal resources to meet the needs of the coastal population in a sustainable way, see e.g., Post and Lundin, 1996), and sustainable coastal development and planning; and is therefore a critical

* Corresponding author.
Email address: ashty.saleem@curtin.edu.au (A. Saleem)

https://doi.org/10.1016/j.catena.2019.03.023
Received 21 September 2018; Received in revised form 9 March 2019; Accepted 17 March 2019
Available online xxx

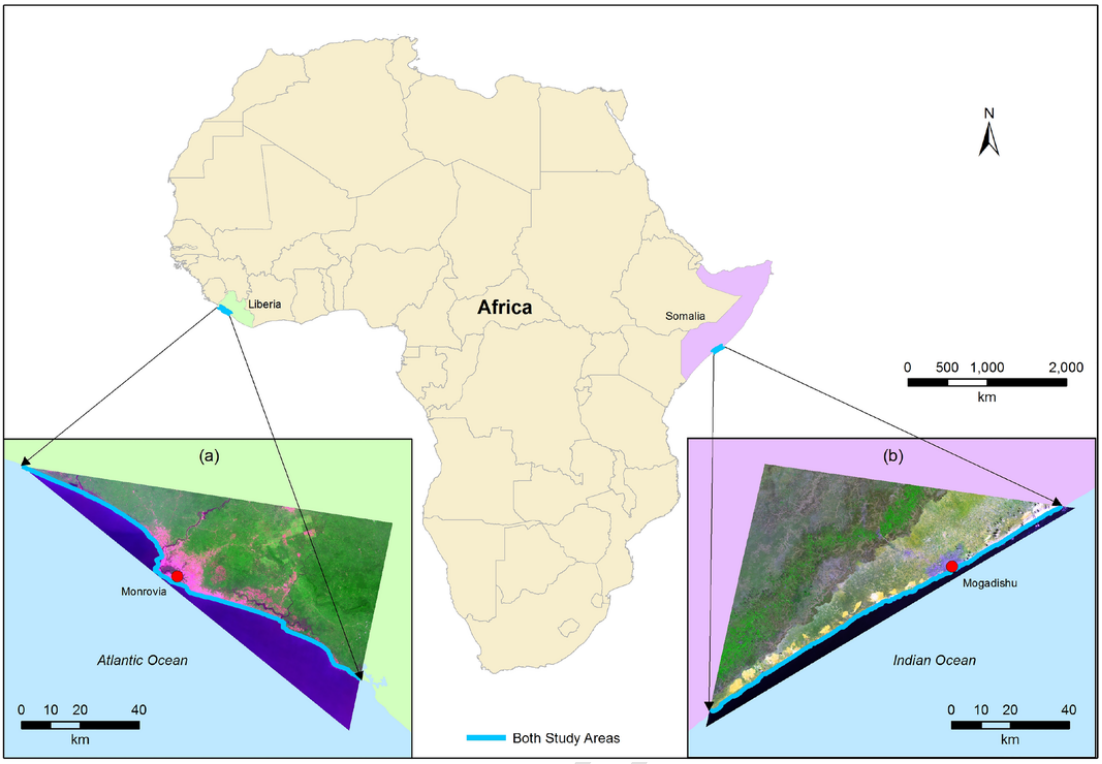

Fig. 1. The map of the study area, (a) the geographical location of Liberia within Africa including Area Of Interest (AOI), and (b) the geographical location of Somalia within Africa including AOI. The base map for both study sites (Liberia and Somalia) is Landsat 8 2014.

Table 1
The final root mean square error (RMSE) for the ground control points (GCPs) during the co-registration process for all images used during this study for both sites ((a) Liberia and (b) Somalia). PAN = panchromatic and MS = multi-spectral.

Sensor	Acquisition date	No. images	No. GCPs	RMSe (pixel/m)
(a)				
Landsat 8 2014/ 2015 PAN	05/01/2015	1	23	0.33/4.95
Landsat 8 2016 PAN	25/12/2016	1	26	0.44/4.40
Landsat 8 2016 MS	25/12/2016	1	28	0.23/6.90
Landsat 8 2017 PAN	28/12/2017	1	21	0.21/3.15
Landsat 8 2017 MS	28/12/2017	1	23	0.35/10.50
Sentinel-2 2015	26/12/2015	3	30	0.20/2.00
Sentinel-2 2016	20/12/2016	3	24	0.15/1.50
Sentinel-2 2017	25/12/2017	3	Reference	NA
Google Earth Pro 2016	2016	NA	NA	NA
(b)				
Landsat 8 2014 PAN	31/01/2014	1	27	0.37/5.55
Landsat 8 2015 PAN	18/01/2015	1	25	0.47/7.05
Landsat 8 2016 MS	22/12/2016	1	22	0.40/12.00
Sentinel-2 2016	6/01/2016	3	29	0.26/2.60
Sentinel-2 2017	10/01/2017	3	32	0.11/1.10
Sentinel-2 2018	10/01/2018	3	Reference	NA
Google Earth Pro 2016	2016	NA	NA	NA

ingredient for decision-making. In light of this, the Metropolitan Borough of Sefton (2002) listed the benefits of coastline evolution information as providing input to coastline review plans, planned maintenance of coastal defenses, achievement of high government level targets, determination of appropriate design criteria for coastal works, bio-diversity action plans, implementation of habitats directive, and leisure and amenity management of shoreline areas. Coastline monitoring, therefore, is economically very important and has attracted many researches globally, see e.g., Gonçalves and Awange (2017) and the references therein.

Traditionally, coastline monitoring have been undertaken using the highly labour intensive and expensive "boots on the ground" surveying methods (see e.g., Gonçalves et al., 2012; Ruggiero et al., 2005; de Schipper et al., 2016; Turner et al., 2016), which are out of reach for most developing countries (see, e.g., Alesheikh et al., 2007; Appeaning Addo et al., 2008; Drapeau and Long, 1984), and also not feasible if the study area is large. From the 1920s, it was demonstrated (see, e.g., Gonçalves and Awange, 2017) that great efficiency gains in coastline mapping (e.g., reduction of expense and labour) could be realized by transitioning from ground-based methods (e.g., plane tables, alidades and stadia rods) to using remotely sensed data (e.g., photogrammetry and aerial imagery interpretation), see e.g., Graham et al. (2003), Parrish et al. (2005), Parrish (2012), Pianca et al. (2015), and Smith Jr (1981). Beginning in the 1970s, when earth observation satellite data became publicly available, further gains in coastline mapping efficiency were enabled (Dolan and Heywood, 1976). Today, satellite imageries are well-established data source for mapping large stretches of coastline in many areas around the world (see e.g., Graham et al., 2003; Graham, 2014; Parrish et al., 2005; Smith Jr, 1981; Stockdon et al., 2002; Yao et al., 2015), with unmanned aerial vehicles (UAVs) and structure from motion also emerging as viable coastal mapping techniques (see e.g., Del Soldato et al., 2018; Westoby et al., 2012; Mancini et al., 2013).

Use of modern remote sensing data sources, e.g., Landsat and ASTER, and GIS analysis, therefore, provide efficient alternative platforms that allows efficient analysis of regions with limited accessibility to be carried out in a sufficient manner (see e.g., Gonçalves and Awange, 2017; Jayson-Quashigah et al., 2013; Yu et al., 2011). These have been demonstrated in studies of coastline monitoring that employ multi-temporal satellite images and Geo-Information System modelling techniques, e.g., in Ghana (Appeaning Addo et al., 2008; Jayson-

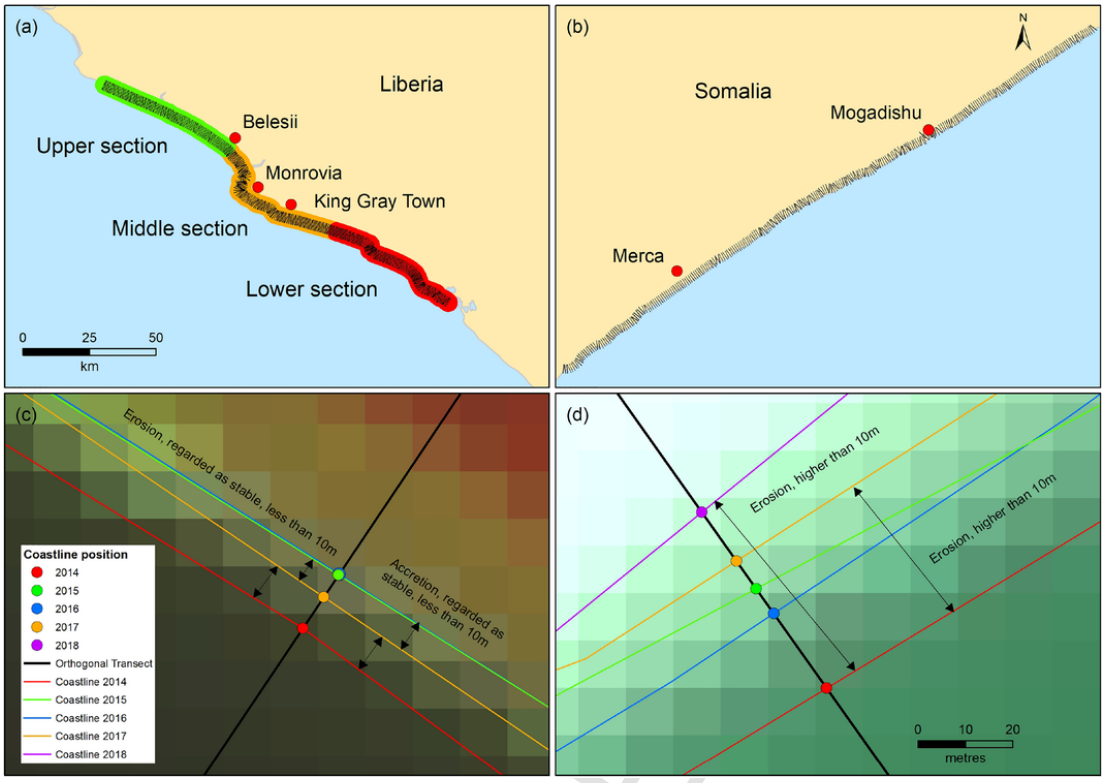

Fig. 2. The locations of the transects for both study area (a) Liberia and (b) Somalia. The figure illustrate the positions of coastlines for different years intersecting points with transect for Liberia (c) and Somalia (d), and how the coastline shifts are considered either as erosion, accretion or stable. The base maps are Sentinel-2 2017 and 2018 for Liberia and Somalia, receptively, with Sentinel-2 used as background.

Quashigah et al., 2013), Bangladesh (Hussain et al., 2014), Thailand (Tochamnanvita and Muttitanon, 2014), Iran (Alesheikh et al., 2007), India (Misra and Balaji, 2015; Poornima and Chinthaparthi, 2014; Rawat and Kumar, 2015), Korea (Shin and Kim, 2015), Egypt (Abd El-Kawy et al., 2011; El-Hattab, 2016), Portugal (Pardo-Pascual et al., 2012), China (Zhang et al., 2013) and more recently for Liberia in Awange et al. (2018). The uses of traditional medium spatial resolution satellite imagery, e.g., Landsat-8 (30 m) is very powerful data for mapping landscape elements at regional scales.

Although, many studies have demonstrated the superb use of the freely available moderate spatio-temporal remotely sensed products for mapping the linear features in the areas where the land is adjacent to water bodies, i.e., shorelines (e.g., Alesheikh et al., 2007; Amaro et al., 2014; Bagli and Soille, 2003; Ekercin, 2007; Guariglia et al., 2006; Kuleli et al., 2011; Li and Gong, 2016; Ouma and Tateishi, 2006; Pardo-Pascual et al., 2012; White and El Asmar, 1999) and rivers morphology studies (Baki and Gan, 2012; Devi et al., 2018; Dewan et al., 2017), using Landsat data at local scale for mapping linear features i.e., shoreline and other coastal zone component i.e., seagrass meadows, however, may not be feasible (Topouzelis et al., 2016) because of its coarse spatial resolution (30 m). For instance, the widely used Landsat products with spatial resolution of 30 m and a temporal resolution of 16 days does not capture the full spectrum of coastline dynamics as demonstrated, e.g., by White and El Asmar (1999). In addition, the use of very high resolution data (VHR) is often limited by high cost on the one hand, and the areal extent of most of the applications on the other hand, thereby putting more emphasis and focus on the freely available high spatio-temporal resolution satellite data. With the launch of the European Sentinel-2 satellite data, with higher temporal (5 days), spectral (13 bands) and spatial (10 m) resolutions, however, a new era for obtaining more accurate coastline shift information to improve our understanding of the coastal dynamics has donned. The availability of Sentinel-2 data with 10 m spatial resolution and 5 days revisit, is expected to improve the mapping accuracy by this new platform in the field of remote sensing (Parrish, 2012; Topouzelis et al., 2016). Since its launch in 2015, Sentinel-2 products have been used, e.g., to map spruce and pine areas in Germany (Immitzer et al., 2018), for land use land cover (LULC) change analysis (Gašparović, 2018; Goldblatt et al., 2018), and its potential for coastal erosion studies acknowledged, e.g., by Awange et al. (2018), Castillo et al. (2017), Hagenaars et al. (2018), and Sagar et al. (2018). The study conducted by Santos and Gonçalves (2014) used Landsat 8 data and Sentinel-2 for testing many applications i.e., LULC, shoreline delineation, and forest mapping. Even with this acknowledged potential (see e.g., Goldblatt et al., 2018), there exists no studies, to the best of the authors' knowledge, that tests manually digitised Sentinel-2's usability for coastline shift monitoring. For instance, although Hagenaars et al. (2018) evaluate the accuracy of automated imagery that included Sentinel-2 for obtaining shoreline positions, its manually digitised version was, however, not assessed. The novelty of this present contribution, therefore, is that it extends on the work of Hagenaars et al. (2018) by providing the first test of the applicability of manually digitised coastline from Sentinel-2 products to monitor coastline movements over data deficient regions, thereby providing high accurate spatio-temporal mapping than previously achieved using freely available remotely sensed Landsat products. The advantages of using manually digitised imagery include, e.g., avoiding misclassification (see Awange et al., 2019; Awange et al., 2018; Dewan et al., 2017). This becomes important for inaccessible regions where obtaining in-situ data for validating automated imageries is impossible as is the case for Somalia. Specifically, the study aims at (i) investigating the suitability of manually digitised Sentinel-2 products within a GIS platform to monitor coastline shift, (ii) assessing the possibility of filling the missing Sentinel-2 gaps with Landsat 8 panchromatic band (15 m) products to provide alternative data source for mapping of

Table 2
Sentinel-2 and Landsat 8 panchromatic band (for infilling of unusable Sentinel-2), which are used in the study for (a) Liberia and (b) Somalia. Some images are used for Liberia's comparative study by using a combination of Sentinel-2, Landsat panchromatic (PAN), and Landsat multi-spectral (MS) images for 2016. The tide is estimated when the satellite overpass both study areas. Note that, L = Landsat, S = Sentinel, Acq. = acquisition, H.T.T. = High Tide Time, L.T.T. = Low Tide Time, H.T. (m) = High Tide, L.T. (m) = Low Tide, and E.T. = Estimated Tide for satellite images. The bolded values in the 8th column (i.e., E.T.) represent the minimum and maximum of the estimated tidal heights for the satellite images and have been used to calculate the differences between these two values. The non-bolded values are same or below the max and min differences and are below 1 m threshold.

Sensor	Acq. date	Acq. time	H.T.T.	L.T.T.	H.T. (m)	L.T. (m)	E.T. (m)
(a)							
L 2014/2015 PAN	05/01/2015	10:58:44	06:41:00	12:43:00	1.16	0.13	0.43
L 2016 PAN	25/12/2016	10:59:11	16:58:00	10:19:00	1.11	0.27	0.35
L 2016 MS	25/12/2016	10:59:11	16:58:00	10:19:00	1.11	0.27	0.35
L 2017 PAN	28/12/2016	10:59:07	14:48:00	08:21:00	1.03	0.29	0.73
L 2017 MS	28/12/2016	10:59:07	14:48:00	08:21:00	1.03	0.29	0.73
S-2 2015	23/12/2015	11:09:08	17:29:00	10:54:00	1.31	0.08	**0.13**
S-2 2015	26/12/2015	11:11:35	07:01:00	13:06:00	1.23	0.05	0.42
S-2 2015	26/12/2015	11:11:35	07:01:00	13:06:00	1.23	0.05	0.42
S-2 2016	17/12/2016	11:01:42	08:53:00	14:57:00	1.17	0.12	0.80
S-2 2016	20/12/2016	11:13:55	11:53:00	05:42:00	0.95	0.38	0.89
S-2 2016	20/12/2016	11:13:55	11:53:00	05:42:00	0.95	0.38	0.89
S-2 2017	25/12/2017	11:05:11	11:05:00	05:19:00	0.92	0.41	**0.92**
S-2 2017	25/12/2017	11:05:11	11:05:00	05:19:00	0.92	0.41	0.92
S-2 2017	25/12/2017	11:05:11	11:05:00	05:19:00	0.92	0.41	0.92
(b)							
L 2014 PAN	31/01/2014	07:12:17	04:15:00	10:42:00	3.12	0.47	**1.91**
L 2015 PAN	18/01/2015	07:11:13	02:17:00	09:07:00	2.72	0.93	1.44
L 2016 MS	6/02/2016	07:11:43	10:23:00	04:35:00	2.00	1.47	1.71
S-2 2016	6/01/2016	07:26:25	01:34:00	08:28:00	2.48	1.18	1.37
S-2 2016	6/01/2016	07:26:25	01:34:00	08:28:00	2.48	1.18	1.37
S-2 2016	6/01/2016	07:26:25	01:34:00	08:28:00	2.48	1.18	1.37
S-2 2017	10/01/2017	07:23:41	02:06:00	08:54:00	2.85	0.85	**1.29**
S-2 2017	10/01/2017	07:23:41	02:06:00	08:54:00	2.85	0.85	1.29
S-2 2017	20/01/2017	07:23:41	09:09:00	03:25:00	2.05	1.4	1.85
S-2 2018	10/01/2018	07:23:17	10:37:00	04:53:00	1.99	1.42	1.67
S-2 2018	10/01/2018	07:23:17	10:37:00	04:53:00	1.99	1.42	1.67
S-2 2018	10/01/2018	07:23:17	10:37:00	04:53:00	1.99	1.42	1.67

coastline shifting where Sentinel-2 data is unusable, e.g., due to cloud cover, and (iii), conducting comparative study over only the Liberian coastal areas using 2016 images of Sentinel-2 (10 m), Landsat panchromatic (15 m) and Landsat multi-spectral (30 m).

To achieve these objectives, Liberia and Somalia, two war-impacted countries (Bastian, 2014) with data deficiency are selected for study during the period 2015–2018. Although it is widely acknowledged that it is essential to validate Sentinel-2 products using field data in order to reinforce and validate its findings, accessing field data can at times prove to be a daunting task as is the case for Liberia and Somalia. In such cases, the use of alternative approaches such as Google Earth Pro has been shown to be reasonable, see, e.g., Hritz (2013). Google Earth Pro provides high-resolution imagery from several commercial satellites from 2000 to the present, see, e.g., Kennedy and Bishop (2011) and Sadr and Rodier (2012). This study uses Liberia and Somalia as case study regions (see Section 2) and pre-tests Sentinel-2 in Section 3. Section 4 discusses the results, and the study is concluded in Section 5.

2. Case study areas and data

2.1. Case study areas

To evaluate the applicability of manually digitised Sentinel-2 products over data deficient regions, Liberia and Somalia, two war impacted countries over the African content were selected and used for coastal shift analysis as case studies. Liberia (West Africa, see Fig. 1), the first coastal section of this study lies between latitudes 4°20′ N and 8°30′ N, and longitudes 7°18′ W and 11°20′ W, and the entire country (has a total of 15 counties subdivided into clans and districts) covers an area of about 111,369 km^2 (LISGIS, 2014) and an estimated population of over 4.5 million people (The World Bank, 2016; UN DESA, 2015). The Liberian coastal zone of about 559 km in length is home to about 58% of the Liberian population (Nicholls and Cazenave, 2010; USAID, 2012). Geographical features along Liberia's coastline include lagoons, sandbars and mangrove swamps (Awange et al., 2018). The topography of Liberia in general is largely flat with the highest point being the top of Mount Wuteve, 1380 m above mean sea level (Awange et al., 2018). The area of interest (AOI) for the present study covers 170 km in length of the Liberia's coast including the capital city Monrovia (Fig. 1a). Regrading the other section of this study (Somalia see Fig. 1b), which is located in the Greater Horn of Africa with a total area of 636,240 km^2, it lies between the latitudes of 1°27′ S and 11°39′ N and between the longitudes of 40°38′ and 51°16′ E. Somalia is typically a dryland country, with low mean annual rainfall (about 282 mm) and arid-land types of soil (Omuto et al., 2014). Broadleaves deciduous trees dominate areas where the mean annual rainfall is greater than 300 mm (Omuto et al., 2014). The AOI is the coastline with a total length of 153 km covering the capital city of Mogadishu along with other coastline areas (see Fig. 1b).

2.2. Data

Sentinel-2 Multispectral Instrument (MSI) was officially launched by ESA on June 23, 2015, with a 5-day temporal resolution (ESA, 2017). Remotely sensed MSI Sentinel-2 products are not just a simple image or photograph taken from space, but made up of many layers of data collected within a wide range of light spectrum that includes, visible (V) to Near-Infrared (NIR) and shortwave Infrared (SWIR) wavelengths. Sentinel-2 systems collect multi-spectral, multi-resolution, and multi-temporal images that can be used for monitoring and understanding human activities on the planet over time (ESA, 2017; USGS, 2015) including coastline shift studies. Also, this remotely sensed

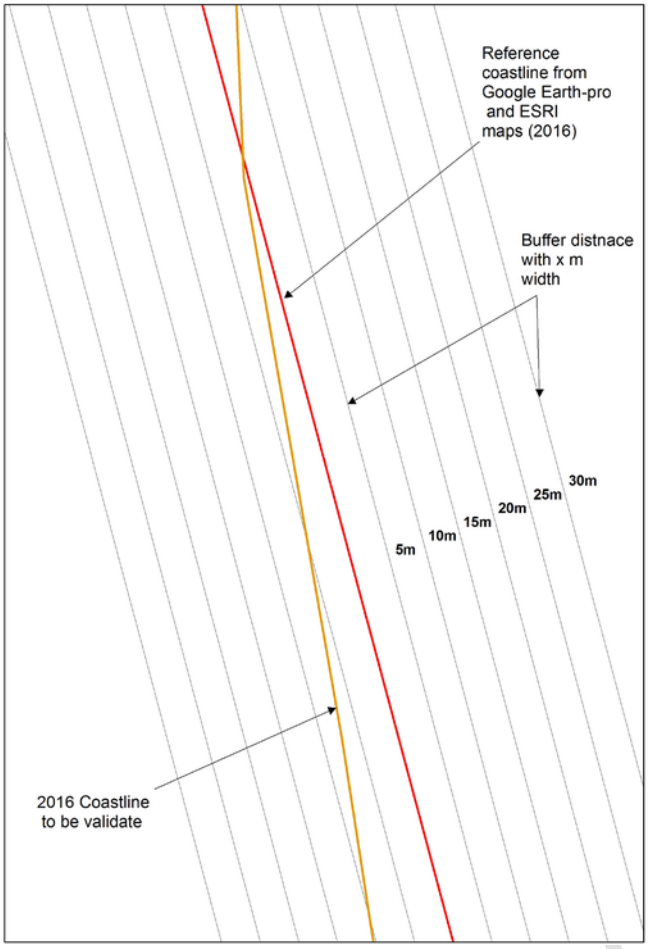

Fig. 3. Validation processes for Sentinel-2 using the 2016 reference data from Google Earth Pro for Liberia coastline by generating different buffer distances from the coastline reference data. This approach was also implemented for Somalia.

Table 3
The percentage of digitised coastline within different buffer distances (metres) from the 2016 reference dataset, which were obtained from Google Earth Pro for Liberia and Somalia. As can be seen from the results, 61% of Liberia's and 62% of Somalia's data meet the threshold of ±10 m. The bolded values in the 3rd column (i.e., 10 m) represent the threshold selected buffer distance for both studies being equivalent to one pixel of Sentinel-2 data.

Country	5 m	**10 m**	15 m	20 m	25 m	30 m
Liberia	33	**61**	71	78	85	87
Somalia	20	**62**	64	68	74	83

dataset can be used to detect, measure and highlight changes in landscape patterns over time because of human activities and natural phenomena. Since changes in the landscape are dynamic, this imagery can be used to study and capture extent of changes at larger scales within short time frames. Sentinel-2 products, which can be freely accessed from United States Geological Survey (USGS) website (`https://earthexplorer.usgs.gov/`) and the official website of the Copernicus Open Access Hub for the European Space Agency (ESA) (`https://scihub.copernicus.eu/`), have the advantages of providing accurate means of mapping and detecting changes where other high resolution products are compounded by cost, time and access constraints. The cooperation between ESA and the USGS provide Level-1C remotely sensed MSI Sentinel-2 products data to end users. This data has been pre-processed to include radiometric and geometric corrections along with ortho-rectification to generate highly accurate geo-located products for researchers (Drusch et al., 2012).

This study uses multitemporal Sentinel-2 and Landsat panchromatic band (also obtained from USGS website (`https://earthexplorer.usgs.gov/`)) to map and analyse the coastline shift of Liberia and Somalia from 2014 to 2017 and 2014 to 2018, respectively, and Landsat MS (30 m) for 2016, see Table 1. The pre-processing steps, i.e., atmospheric correction using Dark Object Subtraction (DOS), image co-registration, image sub-setting and image enhancement are applied on all Sentinel-2 products for both studies areas. DOS method has been recommended, e.g., by Song et al. (2001) as a preferable method as this approach is strictly based on information from the image (Gilmore et al., 2015). For the pre-processing step, Sentinel-2 2017 and 2018 images are used as references to register other images considering Universal Traverse Mercator (UTM) grid zone 29°N and grid zone 38°N for Liberia and Somalia, respectively. During image co-registration process in ArcGIS environment, well distributed ground control points (GCPs) represented by permanent features such as bridges and road intersections are selected (a minimum of 20 GCPs for each image). Using a first order polynomial fit, the co-registration process yield a root mean square error (RMSE) of less than 0.5 pixel for each scene, which corresponds to 5.0, 7.5, and 15 m for Sentinel-2, Landsat panchromatic, and Landsat multi-spectral, respectively (Table 1). Besides the pre-processing step mentioned above, mosaicking process is used for Sentinel-2 data for both studies as three images are required to cover each study area. Regarding Landsat PAN and MS used for the comparative study, these images are co-registered with Sentinel-2 reference images for 2017 (Liberia) and 2018 (Somalia) with RMSE lower than 0.5 pixel (Table 1), where one image is required to cover the study area for both evaluated coastlines. Each image (Sentinel-2, Landsat PAN, and Landsat MS) used during this analysis is finally clipped with AOI vector dataset. For the validation purposes, Google Earth Pro using image slider tool are used for 2016 high resolution image for both case studies (see Table 1).

3. Methods

3.1. Manual digitisation

The coastline from Sentinel-2 and Landsat panchromatic band are delineated using on-screen manual digitisation technique with constant scale of 1:2000 with a single operator. This technique has been proven to be ideal for rivers and coastline extraction by studies such as Dewan et al. (2017) and Salghuna and Bharathvaj (2015). Instantaneous high tidal water lines are used as proxies for coastlines. To be able to calculate the coastline shift or movement as erosion and accretion, orthogonal profiles are generated at an interval of 500 m for both coastal areas using the 2014 extracted coastline shapefile as baseline in ArcGIS environment (Dewan et al., 2017). A total of 345 and 305 transects are generated for Liberia and Somalia coastlines, respectively. The profiles are visually inspected to ensure that they are all orthogonal or perpendicular to the baseline year of 2014 for both regions. Coastline movement of each profile is then calculated for the different periods by calculating the distance between every intersecting coastline with the corresponding transect (Fig. 2). A one pixel shift (and below) for Sentinel-2 10 m, Landsat PAN 15 m and Landsat MS 30 m is regarded as stable (digitising error) for both study areas. Fig. 2 illustrates the process of calculating the coastal shifts and attributing them as stable, accretion, or erosion for all the intersecting transects for both evaluated coastlines. Negative shifts represent coastline erosion whereas positive shifts refer to coastline accretion.

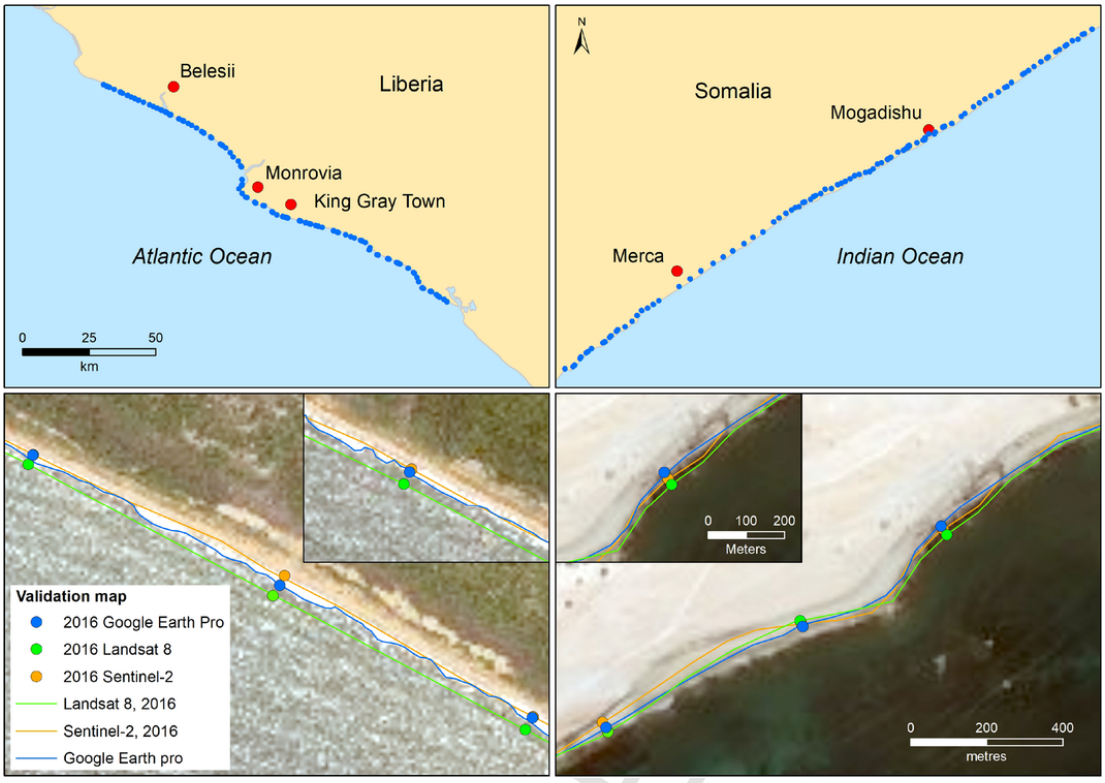

Fig. 4. The location of the ground reference dataset for both study sites, which are zoomed for some selected locations to demonstrate the difference of the Sentinel-2 2016 and Landsat 30 m 2016 coastal positions in respect to the ground reference dataset digitised from Google Earth Pro.

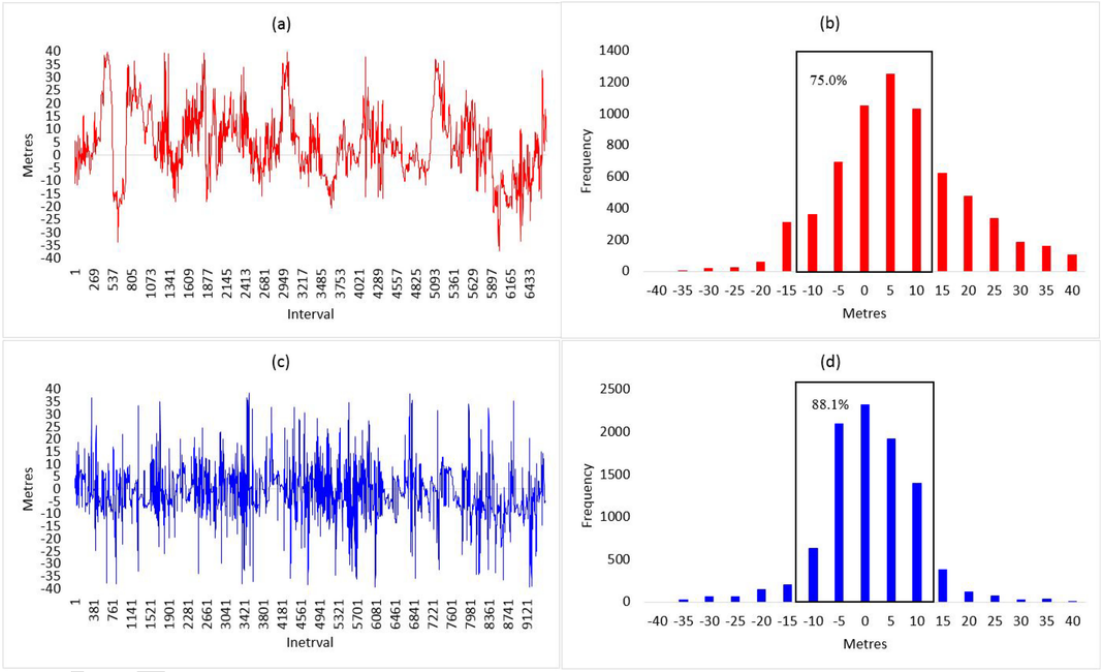

Fig. 5. K-S pre-test of Sentinel-2 products using reference Google Earth Pro data. The figure shows the difference in radial vectors from the origin (a) and normal distribution (b) for Liberia. Figures (c) and (d) represent those of Somalia.

3.2. Pre-test of Sentinel-2 products

To showcase the suitability of Sentinel-2 products in providing useful data for coastal shift analysis, three pre-tests are undertaken; (i) Tidal heights, (ii) Buffer zones, and (iii) Kolmogorov-Smirnov Test. Detailed discussion of these pre-test are presented below.

3.2.1. Tidal heights

For coastal shift analysis studies, it is necessary that all the satellite imagery used during the analysis have the same or close anniversary

Table 4
Kolmogorov-Smirnov (K-S) test result for the 200 randomly selected points for the referent data from Google Earth Pro and Sentinel-2 digitised data for the 2016 images (radial vectors calculation from the origin) for Liberia and Somalia.

Country	Difference	*p*-Value
Liberia	0.082	0.096
Somalia	0.076	0.096

date (same time of year) as much as possible in order to have similar or close range of tidal heights. The close tidal heights among the images used during the coastal shift analysis permit the comparison and calculation of accurate coastal shifting from the remotely sensed data (Santos and Gonçalves, 2014). The tidal heights of the Sentinel-2 data used are checked to ensure that they are below 1 m threshold as suggested by Santos and Gonçalves (2014). To extract accurate planimetric portion of the coastline derived from satellite data, i.e., Sentinel-2 and Landsat 8 PAN, it is essential to estimate the tidal heights from the remotely sensed data during the satellite overpass over the study areas. For Liberia and Somalia regions used herein as case studies, the tidal heights for all images at different satellite overpasses are interpolated using a two-point cosine interpolator (e.g., Santos and Gonçalves, 2014), and the results summarised in Table 2. From these results, since the spatial resolution (pixel size) for Sentinel-2 and Landsat 8 panchromatic band are 10 and 15 m respectively, and the difference between the tidal heights over Liberia from the satellite image is 0.79 m (max-min), and 0.62 m for Somalia, i.e., less than 1 m threshold suggested by Santos and Gonçalves (2014), it is reasonable to conclude that Sentinel-2 and Landsat 8 panchromatic (for infilling of the unusable Sentinel-2 products) images used in this study are adequate for use in coastal shift analysis as they meet the threshold suggested above.

3.2.2. Buffer zones

A positional accuracy from remotely sensed data compared against a reference data can be obtained by calculating the percentage of digitised data that fall within certain buffer distances i.e., a threshold value of one pixel (10 m) for Sentinel-2 data from the reference coastline (Goodchild and Hunter, 1997). This positional accuracy can be achieved by generating different buffer distances around the reference coastline data in ArcGIS environment. To be able to pre-test Sentinel-2 data for coastline shift for both study areas (Liberia and Somalia), the image time slider tool from Google Earth Pro was used to digitise the reference data representing the 2016 high resolution images at constant scales and with a single operator. Google Earth Pro is used to provide reference data due to the fact that collecting field data for both areas was not feasible, and for such long coastlines, enormous time and resources would be required. Use of Google Earth Pro where in-situ "boots on the ground" data are unavailable has been suggested and applied, e.g., by Hritz (2013), Kennedy and Bishop (2011), and Sadr and Rodier (2012). The coastline for the same extends of the study areas are digitised for Liberia and Somalia from Google Earth Pro with total lengths of 170 and 153 km, respectively. After completing the digitisation process for the reference data for both study areas, different buffer distances (5, 10, … and 30 m) are generated for the reference dataset (Fig. 3). The criteria for selecting these buffer distances is the threshold of 10 m buffer distance as the maximum, which is equivalent to one pixel for Sentinel-2 data. The 2016 coastlines for both Liberia and Somalia are digitised from the Sentinel-2 images and intersected with these buffer distances, and percentages of coastline lengths within each buffer distances calculated (see Table 3).

3.2.3. Kolmogorov-Smirnov (K-S) similarity test

Sentinel-2 data, which were digitised from the satellite images are further pre-tested and analysed using Kolmogorov-Smirnov (K-S) similarity statistical test. The Two-sample Kolmogorov-Smirnov test is useful to assess the difference of the empirical cumulative distribution of two samples (Marsaglia et al., 2003). Two samples K-S test can be used to compare two sets of different observations (for this study, the reference from Google Earth Pro and digitised from Sentinel-2 for the 2016 coastline) and check for the similarity in their cumulative distributions (Koc et al., 2018; Massey Jr, 1951). During this test, a maximum absolute differences between two cumulative distributions is calculated and provided to show the maximum differences and their probability statistics being equaled or exceeded (Awange et al., 2016). This maximum difference is compared with the calculated critical *p*-value based on the standard table used for K-S test (Massey Jr, 1951). Both coastline datasets were converted into two points datasets, from which 200 were randomly selected for use as input for the K-S test. The radial vectors from the origin for both datasets (reference and digitised for 2016) were calculated. The test statistics use the maximum absolute difference between two datasets of the distributions, with the difference of the empirical cumulative distributions calculated as (Marsaglia et al., 2003):

$$\mathrm{D} = max_x \left(\mathrm{F}_1(\mathrm{x}) - \mathrm{F}_2(\mathrm{x}) \right), \tag{1}$$

where $F_1(x)$ and $F_2(x)$ are the proportion of the two sample values less than or equal to x, respectively (Marsaglia et al., 2003). The null hypothesis is that the two datasets come from the same distribution, which is rejected at level α (0.05 in this study) if

$$\mathrm{D} > \mathrm{c}(\alpha) \sqrt{\frac{2\mathrm{n}}{\mathrm{n}^2}}, \tag{2}$$

where n is the size of samples, and $c(\alpha)$ calculated as:

$$\mathrm{c}(\alpha) = \sqrt{-\frac{1}{2} \ln\left(\frac{\alpha}{2}\right)}. \tag{3}$$

3.3. Validation

Three comparative analyses are implemented for Sentinel-2 (10 m), Landsat PAN (15 m) and Landsat MS (30 m) over the study areas. For the first one, the coastline for both studies, i.e., Liberia and Somalia are extracted again from Landsat 8 2016 (30 m) with the same constant scale and single operator as used for Sentinel-2 2016 coastal delineation. Traditionally, points from remotely sensed images are normally validated with actual ground points where image pixel coordinates are compared, e.g., to those obtained from global navigation satellite systems (GNSS) (Awange, 2018; Awange, 2012). When such GNSS-based ground reference points are unavailable, alternative procedures such as the use of Google Earth Pro are recommended (e.g., White et al., 2011). In this study, two sets of 100 random points (check points) are generated from the 2016 Sentinel-2 coastline extracted data for Liberia and Somalia. These 100 check points (for each study site) are then used to identify the same locations in Landsat 2016 (30 m) digitised datasets for both case studies (Fig. 4). These 100 check points (Sentinel-2 2016 and Landsat 2016 (30 m)) for both case studies are compared again with the same locations on Google Earth Pro (see, e.g., White et al., 2011; Hare et al., 2018). The differences in their coordinates (i.e., eastings and northings) and other statistical measures, i.e., maximum and minimum differences, mean, standard deviations and Root Mean Square Error (RMSE) are then computed and analysed.

For the second comparative analysis, the coastline of Liberia, 2016 from Sentinel-2, Landsat PAN and Landsat MS are used as an input for the buffer distance pre-test. Finally, another comparative analysis for

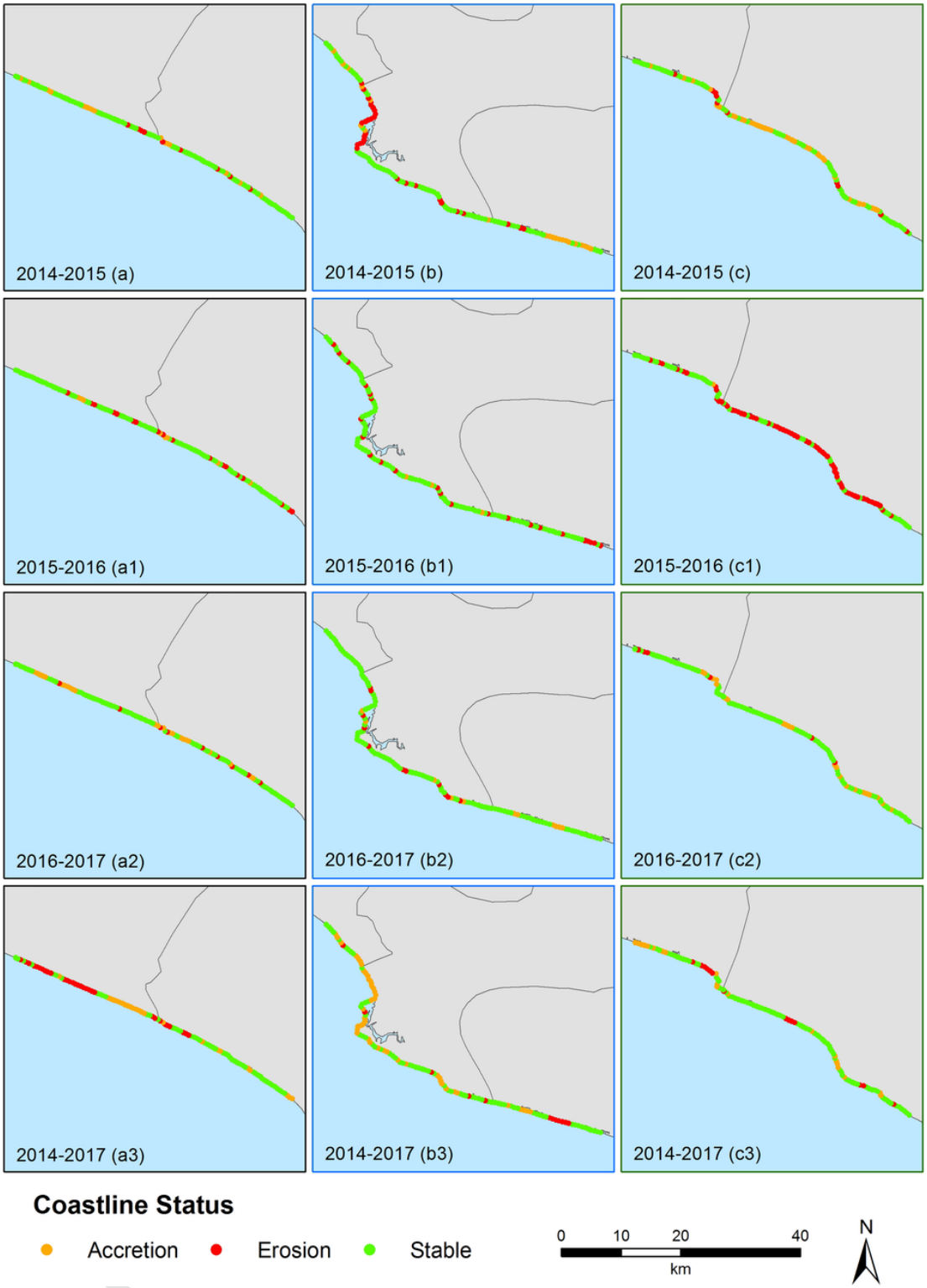

Fig. 6. The spatial patterns of the Liberian coastline, which was divided into three sections for mapping purposes from 2014 to 2017, (a–a3) upper section, (b–b3) middle section, and (c–c3) lower section.

the period 2016–2017 are performed by using only Liberian's coastlines, which are extracted (digitised) from Sentinel-2, Landsat PAN, and Landsat MS. All these comparative analysis are implemented to show the applicability of the Sentinel-2 and Landsat panchromatic over the traditional Landsat MS 30 m pixel size (spatial resolution) for the

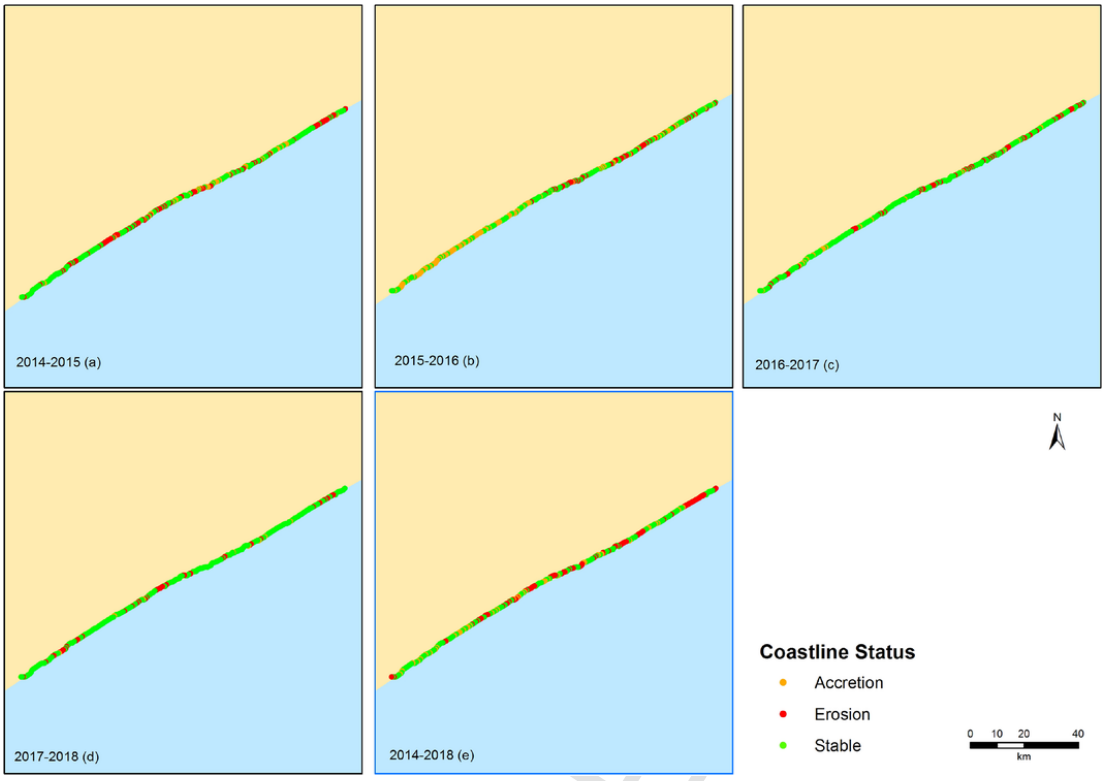

Fig. 7. The spatial patterns of the Somalian coastline from 2014 to 2018. The study covers the periods of (a) 2014–2015, (b) 2015–2016, (c) 2016–2017, (d) 2017–2018, and (e) 2014–2018.

coastal delineation and shift studies. As stated earlier, Landsat PAN is tested for its potential to fill in gaps in Sentinel-2.

4. Results and discussion

4.1. Pre-test results

The pre-test results of Section 3 using different approaches i.e., tidal heights, buffer distances, and K-S test showcase the suitability of using Sentinel-2 data for mapping linear features and coastal shifts for both evaluated case studies. Such pre-test have been recommended/undertaken, e.g., in Awange et al. (2016), Goodchild and Hunter (1997), Koc et al. (2018), and Santos and Gonçalves (2014). This analysis show more than 60% of the total length of the digitised data falling within the 10 m threshold from the reference dataset for both Liberia and Somalia, thus aligning with the spatial resolution of one pixel for Sentinel-2 data (Table 3). This implies that more than 60% of the Sentinel-2 data used in both regions meet the required threshold.

The K-S pre-test shows that the largest percentage of the evaluated datasets (Fig. 5) fall within the ±10 m for both studies (75.0% and 88.1% for Liberia and Somalia, respectively). This indicates that both dataset are similar and normally distributed based on the statistics results, i.e., K-S test (Table 4). The critical *p*-value for both cases from the 200 random samples is 0.096. Since the maximum difference values (0.082 and 0.076 for Liberia and Somalia, respectively) are lower than the *p*-values, both datasets (reference and digitised) for Liberia and Somalia are statistically similar to the reference data generated from Google Earth Pro and normally distributed (Table 4).

From the K-S pre-test results in Fig. 5, Sentinel-2 product used herein is further established to be suitable for coastal shift studies since they fall within ±10 m, which is aligned with the threshold of 1-pixel for Sentinel-2 used during this evaluation for both study areas. Again, this test showcases the suitability of Sentinel-2 data used in this study for mapping the linear feature, i.e., coastline at regional scale.

4.2. Coastal shift results

4.2.1. Liberia

For the Liberian coastal areas, the transects analysis results show the coastal stability above 57% (Fig. 8a) during the overall period 2014–2017 followed by accretion and then erosion in the upper section (Fig. 6a–a3) compared to the middle and lower portions of the coastline. This erosion could be due to the impacts of climate change, e.g., sea level rise (Williams, 2016) and sand mining along the coastal zone of Liberia (Awange et al., 2018; UNDP, 2006; Wiles, 2005). For the 2014–2015 period (Fig. 6b), the middle portion of coastline experienced more erosion than other parts as a result of the illegal mangrove logging and sand mining (El-Hattab, 2016; Liberia, 2016; UNEP, 2004; Wiles, 2005). Also, floods from river mouth, which crosses the capital city of Liberia (middle section) or other climate change factors, i.e., sea level rise (Awange et al., 2018; El-Hattab, 2016; Werrell and Femia, 2014) could be contributing to the erosion. Furthermore, sand mining and mangrove logging (Awange et al., 2018; UNDP, 2006; Siakor, 2014) could also be involved as this pattern is not visible in other parts of the study during the evaluated period (see, Fig. 6b–b3). For the 2015–2016 period, there are many transects that show more erosion than accretion. This may be related to the rivers and estuaries activities along the coastal zone of Liberia (Awange et al., 2018) and sea level rise as predicted by Wiles (2005). Other factors such as subsidence have also been reported as possible causes of sea level rise (see, e.g., Brown et al., 2011; Dasgupta et al., 2009; Hinkel et al., 2012), which may at the same time have a direct effect for causing erosion in the coastal regions of Liberia (UNEP, 2004; Wiles, 2005).

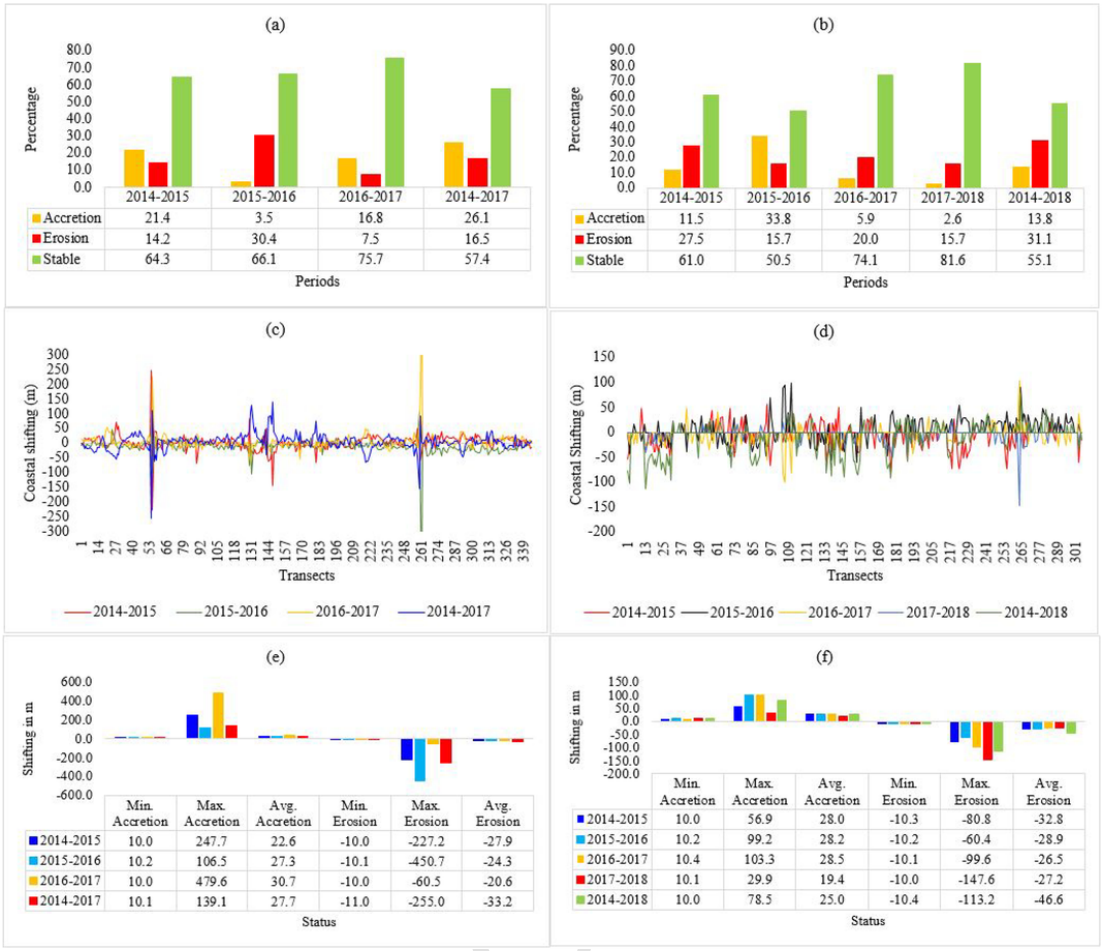

(a)

	2014-2015	2015-2016	2016-2017	2014-2017
Accretion	21.4	3.5	16.8	26.1
Erosion	14.2	30.4	7.5	16.5
Stable	64.3	66.1	75.7	57.4

(b)

	2014-2015	2015-2016	2016-2017	2017-2018	2014-2018
Accretion	11.5	33.8	5.9	2.6	13.8
Erosion	27.5	15.7	20.0	15.7	31.1
Stable	61.0	50.5	74.1	81.6	55.1

(e)

	Min. Accretion	Max. Accretion	Avg. Accretion	Min. Erosion	Max. Erosion	Avg. Erosion
2014-2015	10.0	247.7	22.6	-10.0	-227.2	-27.9
2015-2016	10.2	106.5	27.3	-10.1	-450.7	-24.3
2016-2017	10.0	479.6	30.7	-10.0	-60.5	-20.6
2014-2017	10.1	139.1	27.7	-11.0	-255.0	-33.2

(f)

	Min. Accretion	Max. Accretion	Avg. Accretion	Min. Erosion	Max. Erosion	Avg. Erosion
2014-2015	10.0	56.9	28.0	-10.3	-80.8	-32.8
2015-2016	10.2	99.2	28.2	-10.2	-60.4	-28.9
2016-2017	10.4	103.3	28.5	-10.1	-99.6	-26.5
2017-2018	10.1	29.9	19.4	-10.0	-147.6	-27.2
2014-2018	10.0	78.5	25.0	-10.4	-113.2	-46.6

Fig. 8. The result of the coastline shift analysis for Liberia (2014–2017) and Somalia (2014–2018). (a) and (b), show the prearranges of transects that experienced either accretion, erosion (higher than 10 m) or stability (below ±10 m) for Liberia and Somalia, respectively. (c) and (d), show the plot of the coastline behaviour with time for Liberia and Somalia, respectively. (e) and (f), show the average of accretion and erosion for the coastlines with times for Liberia and Somalia, respectively.

4.2.2. Somalia

For the Somalian coastal areas, the transects analysis results show the coastal areas to have maintained their stability above 50% (Fig. 8b) during the overall study period 2014–2018 followed by erosion and then accretion over the evaluated coastline areas (Fig. 7). The erosion may also be due to the impacts of climate change, e.g., sea level rise and tree logging, especially for the coastal zones (Bolognesi et al., 2015). For the overall period 2014–2018 (Fig. 7e), the coastline experienced more erosion as a result of tree logging and losing mangrove cover (Bolognesi and Leonardi, 2018). Also, this erosion could be related to other factors such as climate change (Nicholls and Cazenave, 2010) and subsidence (see, e.g., Brown et al., 2011; Dasgupta et al., 2009; Hinkel et al., 2012), which may be the same case as Liberia where after losing the vegetation cover, the coastal areas become very vulnerable to erosion (Awange et al., 2018; Wiles, 2005).

4.3. Comparison of the case studies

In light of the pre-test approaches, shoreline mapping is undertaken for different years using Sentinel-2 and Landsat 8 panchromatic band for Liberia (2014–2017) and Somalia (2014–2018) and the results presented in Figs. 6 and 7, respectively. From these results, the coastal areas for both locations can be regarded in general as stable since the majority of the transects used during the coastal analysis show that the coastlines maintained their stability (always above 50%, see, Fig. 7a and b).

The coastal shift analysis for the Liberian and Somalian regions presented in panels c and d in Fig. 8 show negative and positive shifting patterns that occurred during the evaluated periods. These figures show in general that the coastline of Liberia is more dynamic than that of Somalia, which experienced more erosion in three dynamic sections (Awange et al., 2018). This may be due to the fact that the coastline of Liberia, as mentioned before, is affected by the crossing estuaries and rivers making them very vulnerable to erosion especially after losing mangrove because of the human activities, i.e., illegal logging (Wiles, 2005). The coastal zones for Somalia experienced more erosion than accretion especially for the overall period (2014–2018) most likely due to sea level rise (Nicholls and Cazenave, 2010) and illegal logging for charcoal production that makes it more vulnerable to erosion (Bolognesi and Leonardi, 2018).

4.4. Validation results

To be able to showcase further the preferability and suitability of using Sentinel-2 (MSI) over the Landsat MS (30 m pixel) products, a comparative study was implemented as mentioned in Section 3. The results of this comparative study (Sentinel-2 and Landsat multilateral (30 m)) indicate that an improvement is gained by using Sentinel-2 over the traditional Landsat (30 m), i.e., 23% on average (32% for Liberia and 14% for Somalia). Comparing 100 check points with

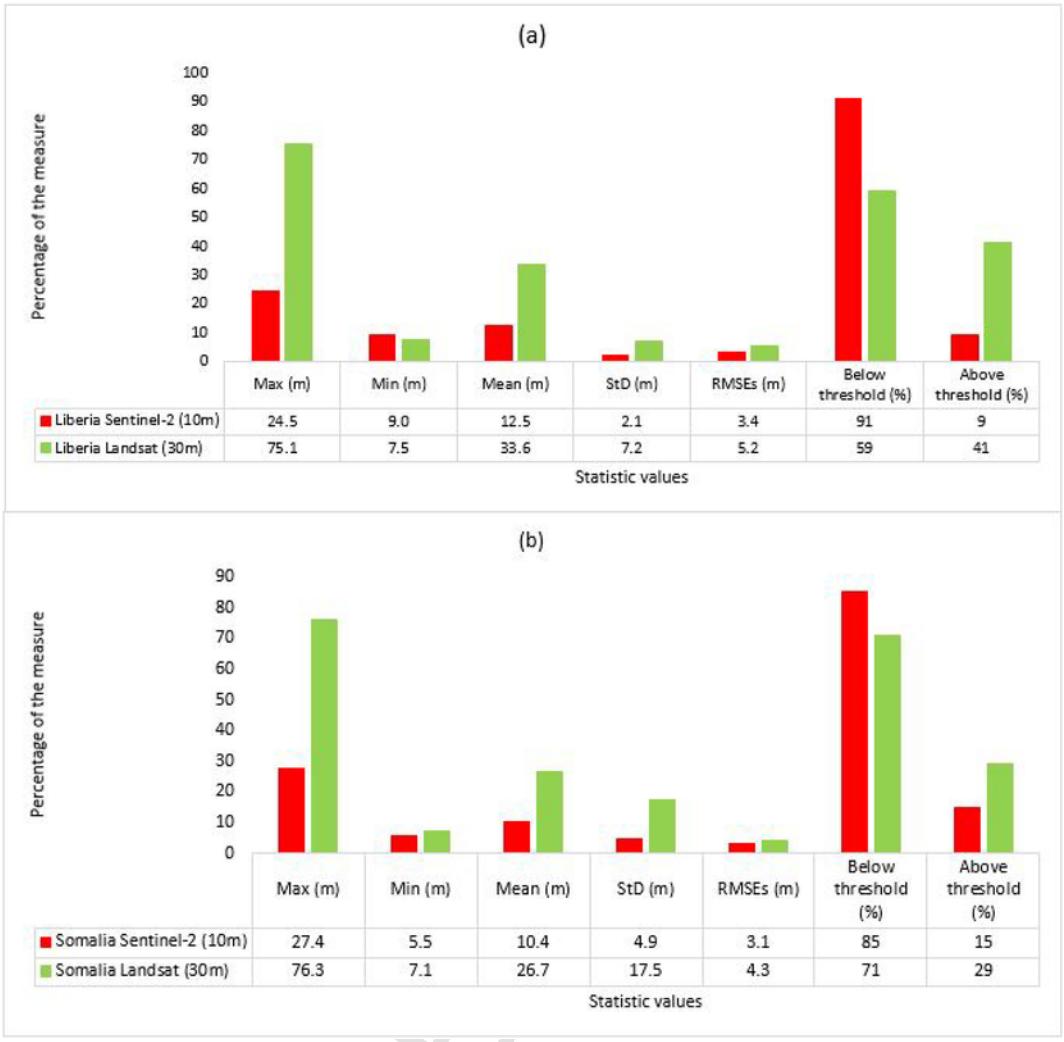

Fig. 9. The statistical measures of accuracies for 100 check points for the 2016 Sentinel-2 data and Landsat 8 30 m data compared with Google Earth Pro (a) Liberia and (b) Somalia.

Table 5
The percentage of digitised coastline for Sentinel-2, Landsat Panchromatic (Pan), and Landsat Multi-Spectral (MS) for 2016 within different buffer distances (metres) from the 2016 reference dataset, which were obtained from Google Earth Pro for Liberia. As can see from the results, 61% of Sentinel-2 and 53% of Landsat Panchromatic and 27% of Landsat Multi-spectral data meet the ±10 m threshold. The bolded values in the 3rd column (i.e., 10 m) represent the threshold selected buffer distance for Liberia being equivalent to one pixel of Sentinel-2 data.

Satellite image	5 m	**10 m**	15 m	20 m	25 m	30 m
Sentinel-2 10 m	33	**61**	71	78	85	87
Landsat 8 (Pan) 15 m	30	**53**	68	77	83	87
Landsat 8 (MS) 30 m	10	**27**	55	60	67	72

Google Earth Pro (i.e., surrogate in-situ reference data) indicate 91% agreement for Liberia and 85% for Somalia (Fig. 9a and b). These results indicate the potential of using Sentinel-2 data for future coastal studies over Landsat MS data 30 m resolution, particularly for the data deficient regions when higher accurate results are required. In addition, the panchromatic band with 15 m pixel size provides relevant data that can complement the missing data for Sentinel-2 when cloud is present (Santos and Gonçalves, 2014; Topouzelis et al., 2016).

Finally, two other comparative analysis are implemented (buffer distance and period analysis 2016–2017) for Sentinel-2 (10 m), Landsat PAN (15 m) and Landsat MS (30 m) for the 2016 and 2017 images over the coastal study areas of Liberia. The analysis of the buffer distance show again the suitability of the Sentinel-2 and Landsat PAN over the Landsat MS, i.e., the percentages of Sentinel-2 and Landsat PAN data falling within 10 m threshold is much higher than Landsat MS by 35% and 26%, respectively (see, Table 5). For the final comparative analysis of the Liberia coastlines extracted from the 2016 and 2017 images for sentinel-2, Landsat PAN, and Landsat MS show that the first two data (images) can capture similar coastline shift and same coastal behaviour (see, Fig. 10a) when compared with Landsat MS 30 m. The peaks which are shown in the figure are the areas with high erosion or accretion for both case studies.

5. Conclusions

The study aimed at evaluating the potential of using Sentinel-2 remotely sensed data for coastal shift studies on the one hand, and complementing it with Landsat 8 PAN (15 m) on the other hand. Furthermore, the study compared Sentinel-2, Landsat PAN and Landsat MS to assess the suitability of the former over the later and the possibility of infilling the Sentinel-2 gaps. Liberia and Somalia, two war-impacted and data deficient regions were selected as case studies. First, before employing the Sentinel-2 data for coastal shift study over Liberia and Somalia, they were pre-tested using tidal heights, buffer zones, and K-S similarity tests. The outcomes of pre-testing indicated that Sentinel-2

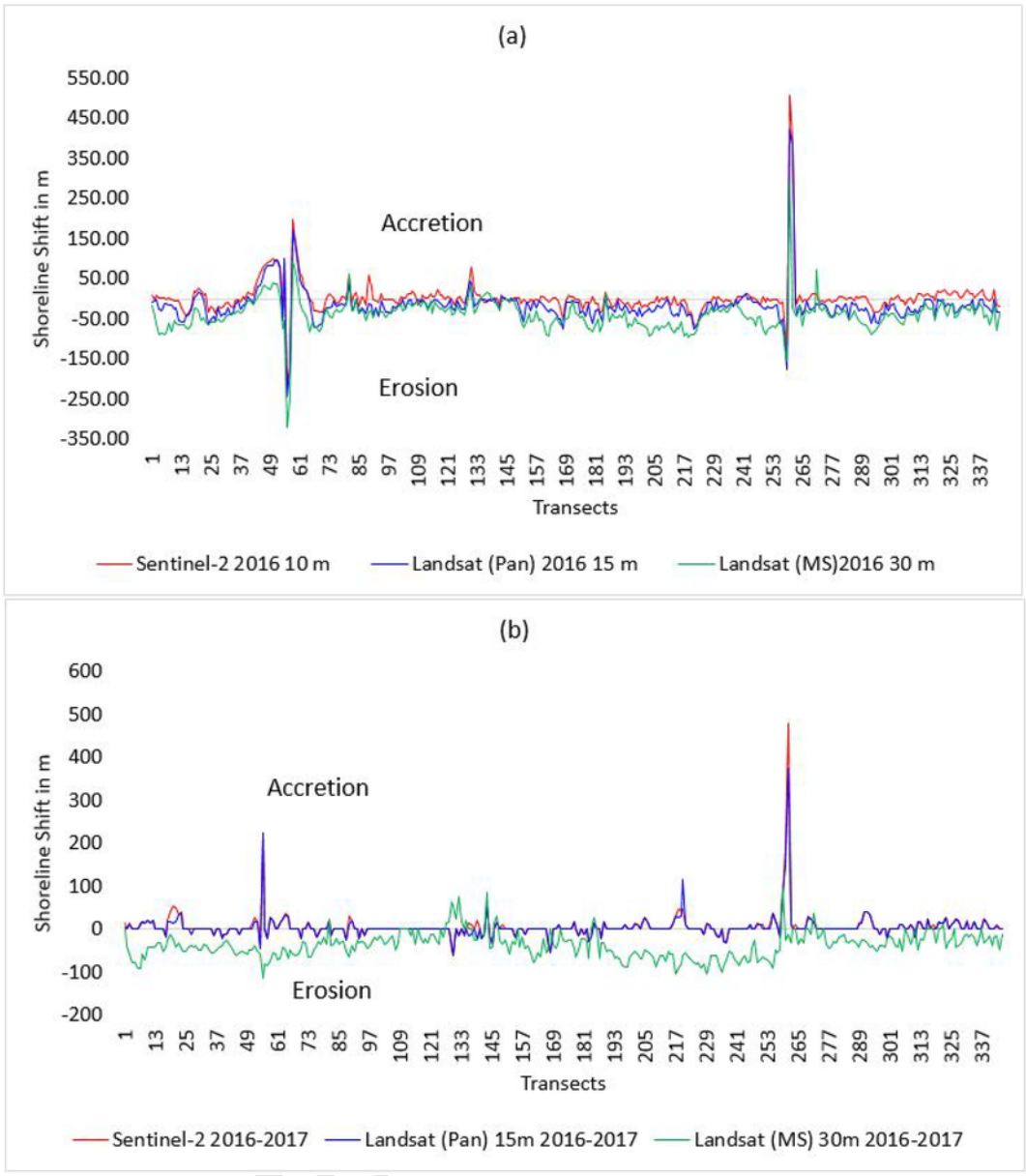

Fig. 10. (a) The extracted Liberian's coastal zones from Sentinel-2, Landsat Panchromatic, and Landsat multi-spectral for 2016 images. (b) The coastal shift for the two-year period (2016–2017) of Sentinel-2, Landsat panchromatic and Landsat multi-spectral showing the similarity between Sentinel-2 and Landsat PAN compared to Landsat multi-spectral in coastal mapping. The peaks which are showing the figure are the areas with high erosion or accretion for both case studies.

data met the 10 m pixel size threshold thereby rendering them applicable for further use in studying the coastal shift dynamics of the Liberian and Somalian coasts. Following the application of Sentinel-2 over these two case study regions, the most important findings of this study are:

- Compared to 100 randomly selected Landsat 8 (30 m) check points, Sentinel-2 provided 23% (on average) improvement (32% for Liberia and 14% for Somalia),
- Buffer distance and period analysis 2016–2017 for Sentinel-2 (10 m), Landsat PAN (15 m) and Landsat MS (30 m) show again the suitability of the Sentinel-2 and Landsat PAN over the Landsat MS products, where they capture more detailed coastline shift over the Landsat MS 30 m.
- Landsat 8 panchromatic band data is suitable for complementing Sentinel-2 products when data is missing or unavailable, e.g., due to cloud cover. This was achieved by using the cross reference of Sentinel-2 and Landsat panchromatic band data to cover the missing data, i.e., using 2015 Landsat as replacement for Sentinel-2 for Somalia because of cloud cover where 53% of the data were found to meet the threshold.
- There exist potential of using Sentinel-2 data source for coastline shift analysis monitoring study, particular for data deficient countries such as Liberia and Somalia with limited remote sensing resources capability.

Uncited reference

UNDP, 2015

Acknowledgment

Dr. Ashty Saleem is grateful for the opportunity offered to him by Curtin University to undertake his postdoctoral studies.

References

Abd El-Kawy, O.R., Rød, J.K., Ismail, H.A., Suliman, A.S., 2011. Land use and land cover change detection in the western Nile delta of Egypt using remote sensing data. Appl. Geogr. 31 (2), 483–494. https://doi.org/10.1016/j.apgeog.2010.10.012.

Alesheikh, A.A., Ghorbanali, A., Nouri, N., 2007. Coastline change detection using remote sensing. Int. J. Environ. Sci. Technol. 4 (1), 61–66. https://doi.org/10.1007/bf03325962.

Amaro, V.E., Gomes, L.R.S., de Lima, F.G.F., Scudelari, A.C., Neves, C.F., Busman, D.V., Santos, A.L.S., 2014. Multitemporal analysis of coastal erosion based on multisource satellite images, Ponta Negra Beach, Natal City, Northeastern Brazil. Mar. Geod. 38 (1), 1–25. https://doi.org/10.1080/01490419.2014.904257.

Appeaning Addo, K., Walkden, M., Mills, J.P., 2008. Detection, measurement and prediction of shoreline recession in Accra, Ghana. ISPRS J. Photogramm. Remote Sens. 63 (5), 543–558. https://doi.org/10.1016/j.isprsjprs.2008.04.001.

Awange, J., 2018. Environmental monitoring. In: GNSS Environmental Sensing. Environmental Science and Engineering. Springer, Cham.

Awange, J., Saleem, A., Konneh, S., Gonçalves, R., Kiema, J.B.K., Hu, K., 2018. Liberia's coastal erosion vulnerability and LULC change analysis: post-civil war and Ebola epidemic. Appl. Geogr.(Revised).

Awange, J.L., 2012. Environmental Monitoring Using GNSS: Global Navigation Satellite Systems. Springer Science & Business Media.

Awange, J.L., Saleem, A., Sukhadiya, R.M., Ouma, Y.O., Kexiang, H., 2019. Physical dynamics of Lake Victoria over the past 34 years (1984–2018): is the lake dying?. Sci. Total Environ. 658, 199–218.

Awange, Joseph L., Mpelasoka, Freddie, Gonçalves, Rodrigo M., 2016. When every drop counts: analysis of droughts in Brazil for the 1901–2013 period. Sci. Total Environ. 566, 1472–1488.

Bagli, S., Soille, P., 2003. Morphological automatic extraction of Pan-European coastline from Landsat ETM + images. In: International Symposium on GIS and Computer Cartography for Coastal Zone Management. pp. 256–269, October.

Baki, A.B.M., Gan, T.Y., 2012. Riverbank migration and island dynamics of the braided Jamuna River of the Ganges–Brahmaputra basin using multi-temporal Landsat images. Quat. Int. 263, 148–161.

Bastian, M., 2014. Ebola-hit Liberia on brink of societal collapse – experts. Rappleravailable on http://www.rappler.com/world/regions/africa/70583-ebola-hit-liberia-societal-breakdown, (November 2016).

Bolognesi, M., Leonardi, U., 2018. Analysis of Very High-Resolution Satellite Images to Generate Information on the Charcoal Production and Its Dynamics in South Somalia from 2011 to 2017.

Bolognesi, M., Vrieling, A., Rembold, F., Gadain, H., 2015. Rapid mapping and impact estimation of illegal charcoal production in southern Somalia based on WorldView-1 imagery. Energy Sustain. Dev. 25, 40–49.

Brown, S., Kebede, A.S., Nicholls, R.J., 2011. Sea-Level Rise and Impacts in Africa, 2000 to 2100. School of Civil Engineering and the Environment University of Southampton, UK.

Castillo, J.A.A., Apan, A.A., Maraseni, T.N., Salmo III, S.G., 2017. Estimation and mapping of above-ground biomass of mangrove forests and their replacement land uses in the Philippines using Sentinel imagery. ISPRS J. Photogramm. Remote Sens. 134, 70–85.

Dasgupta, S., Laplante, B., Murray, S., Wheeler, D., 2009. Climate Change and the Future Impacts of Storm-Surge Disasters in Developing Countries.

Del Soldato, M., Riquelme, A., Tomás, R., De Vita, P., Moretti, S., 2018. Application of Structure From Motion Photogrammetry to Multi-Temporal Geomorphological Analyses: Case Studies From Italy and Spain.

Devi, D., Phukan, N., Sarma, B., 2018. A study of erosional depositional activity and land use mapping of Majuli River island using Landsat data. In: Hydrologic Modeling. Springer, Singapore, pp. 187–200.

Dewan, A., Corner, R., Saleem, A., Rahman, M.M., Haider, M.R., Rahman, M.M., Sarker, M.H., 2017. Assessing channel changes of the Ganges-Padma River system in Bangladesh using Landsat and hydrological data. Geomorphology 276, 257–279. https://doi.org/10.1016/j.geomorph.2016.10.017.

Di, K., Ma, R., Wang, J., Li, R., 2003. Coastal mapping and change detection using high-resolution IKONOS satellite imagery. In: Proceedings of the 2003 Annual National Conference on Digital Government Research. ACM InternationalConference Proceeding Series, vol. 130, Digital Government Society of North America, Boston, MA, pp. 1–4.

Dolan, R., Heywood, J., 1976. Landsat application of remote sensing to shoreline-form analysis. In: NASA Technical Report, NASA Goddard Space Flight Center, Greenbelt, Maryland. p. 33.

Drapeau, G., Long, B., 1984. Measurements of bedload transport in the nearshore zone using radioisotopic sand tracers. Coastal Engineering Proceedings 1 (19).

Drusch, M., Del Bello, U., Carlier, S., Colin, O., Fernandez, V., Gascon, F., Hoersch, B., Isola, C., Laberinti, P., Martimort, P., 2012. Sentinel-2: ESA's optical high-resolution mission for GMES operational services. Remote Sens. Environ. 120, 25–36.

Ekercin, S., 2007. Coastline change assessment at the Aegean Sea coasts in Turkey using multitemporal Landsat imagery. J. Coast. Res. 691–698.

El-Hattab, M.M., 2016. Applying post classification change detection technique to monitor an Egyptian coastal zone (Abu Qir bay). The Egyptian Journal of Remote Sensing and Space Science 19, 23–36. https://doi.org/10.1016/j.ejrs.2016.02.002.

ESA, 2017. European Space Agency, Copernicus Open Access Hub. SERCO.

Gašparović, M., Jogun, T., 2018. The effect of fusing Sentinel-2 bands on land-cover classification. Int. J. Remote Sens. 39 (3), 822–841.

Gilmore, S., Saleem, A., Dewan, A., 2015. Effectiveness of DOS (dark-object subtraction) method and water index techniques to map wetlands in a rapidly urbanising megacity with Landsat 8 data. In: Research@ Locate'15. pp. 100–108 http://SunSITE, (Informatik. RWTH-Aachen. DE/Publications/CEUR-WS/).

Goldblatt, R., Deininger, K., Hanson, G., 2018. Utilizing publicly available satellite data for urban research: mapping built-up land cover and land use in Ho Chi Minh City, Vietnam. Dev. Eng. 3, 83–99.

Gonçalves, R.M., Awange, J.L., 2017. Evaluation of the three most widely-used GNSS-based shoreline monitoring methods to support integrated coastal zone management policies. J. Surv. Eng.

Gonçalves, R.M., Awange, J., Krueger, C.P., 2012. GNSS-based monitoring and mapping of shoreline position in support of planning and management of Matinhos/PR (Brazil). J. Glob. Position. Syst. 11 (1), 156–168.

Goodchild, M.F., Hunter, G.J., 1997. A simple positional accuracy measure for linear features. Int. J. Geogr. Inf. Sci. 11 (3), 299–306.

Graham, D., Sault, M., Bailey, J., 2003. National ocean service shoreline: past, present, and future. J. Coast. Res. (38), 14–32, Special Issue No..

Graham, K., 2014. Liberia's losing battle with erosion and rising sea levels. Environmentavailable on http://www.digitaljournal.com/news/environment/liberia-s-losing-battle-with-erosion-and-rising-sea-levels/article/392869, (November, 2016).

Guariglia, A., Buonamassa, A., Losurdo, A., Saladino, R., Trivigno, M.L., Zaccagnino, A., Colangelo, A., 2006. A multisource approach for coastline mapping and identification of shoreline changes. Ann. Geophys. (1), 49.

Hagenaars, G., de Vries, S., Luijendijk, A.P., de Boer, W.P., Reniers, A.J., 2018. On the accuracy of automated shoreline detection derived from satellite imagery: a case study of the sand motor mega-scale nourishment. Coast. Eng. 133, 113–125.

Hare, T.M., Rossi, A.P., Frigeri, A., Marmo, C., 2018. Interoperability in planetary research for geospatial data analysis. Planet. Space Sci. 150, 36–42.

Hinkel, J., Brown, S., Exner, L., Nicholls, R.J., Vafeidis, A.T., Kebede, A.S., 2012. Sea-level rise impacts on Africa and the effects of mitigation and adaptation: an application of DIVA. Reg. Environ. Chang. 12 (1), 207–224.

Hritz, C., 2013. A malarial-ridden swamp: using Google Earth Pro and Corona to access the southern Balikh Valley, Syria. J. Archaeol. Sci. 40 (4), 1975–1987.

Hussain, M.A., Tajima, Y., Gunasekara, K., Rana, S., Hasan, R., 2014. Recent coastline changes at the eastern part of the Meghna estuary using PALSAR and Landsat images. IOP Conf. Ser. Earth Environ. Sci. 20, 012047. https://doi.org/10.1088/1755-1315/20/1/012047.

Immitzer, M., Böck, S., Einzmann, K., Vuolo, F., Pinnel, N., Wallner, A., Atzberger, C., 2018. Fractional cover mapping of spruce and pine at 1 ha resolution combining very high and medium spatial resolution satellite imagery. Remote Sens. Environ. 204, 690–703.

Jayson-Quashigah, P.-N., Addo, K.A., Kodzo, K.S., 2013. Medium resolution satellite imagery as a tool for monitoring shoreline change. Case study of the eastern coast of Ghana. J. Coast. Res. 65, 511–516. https://doi.org/10.2112/si65-087.1.

Kennedy, D., Bishop, M.C., 2011. Google Earth and the archaeology of Saudi Arabia. A case study from the Jeddah area. J. Archaeol. Sci. 38 (6), 1284–1293.

Koc, C.B., Osmond, P., Peters, A., Irger, M., 2018. Understanding land surface temperature differences of local climate zones based on airborne remote sensing data. IEEE J-STARS

Kuleli, T., Guneroglu, A., Karsli, F., Dihkan, M., 2011. Automatic detection of shoreline change on coastal Ramsar wetlands of Turkey. Ocean Eng. 38 (10), 1141–1149.

Li, R., Weng, K.C., Willis, D., 1998. A coastal GIS for shoreline monitoring and management — case study in Malaysia. SaLIS 58 (3), (157–166).

Li, W., Gong, P., 2016. Continuous monitoring of coastline dynamics in western Florida with a 30-year time series of Landsat imagery. Remote Sens. Environ. 179, 196–209.

Liberia, 2016. Countries. available on http://www.illegal-logging.info/regions/liberia, (November, 2016).

LISGIS, 2014. Liberia demographic and health survey 2013. available on https://dhsprogram.com/pubs/pdf/FR291/FR291.pdf, (November, 2016).

Mancini, F., Dubbini, M., Gattelli, M., Stecchi, F., Fabbri, S., Gabbianelli, G., 2013. Using unmanned aerial vehicles (UAV) for high-resolution reconstruction of topography: the structure from motion approach on coastal environments. Remote Sens. 5 (12), 6880–6898.

Marsaglia, G., Tsang, W., Wang, J., 2003. Evaluating Kolmogorov's distribution. J. Stat. Softw. 8 (18).

Massey Jr, F.J., 1951. The Kolmogorov-Smirnov test for goodness of fit. J. Am. Stat. Assoc. 46 (253), 68–78.

Metropolitan Borough of Sefton, 2002. Shoreline monitoring annual report 2001/2002. In: http://www.sefton.gov.uk/pdf/TS_cdef_monitor_20012.pdf.

Misra, A., Balaji, R., 2015. A study on the shoreline changes and land-use/land-cover along the South Gujarat coastline. Procedia Eng. 116, 381–389. https://doi.org/10.1016/j.proeng.2015.08.311.

Nicholls, R.J., Cazenave, A., 2010. Sea-level rise and its impact on coastal zones. Science 328 (5985), 1517–1520. https://doi.org/10.1126/science.1185782.

Omuto, C.T., Balint, Z., Alim, M.S., 2014. A framework for national assessment of land degradation in the drylands: a case study of Somalia. Land Degrad. Dev. 25 (2), 105–119.

Ouma, Y.O., Tateishi, R., 2006. A water index for rapid mapping of shoreline changes of five East African Rift Valley lakes: an empirical analysis using Landsat TM and ETM + data. Int. J. Remote Sens. 27 (15), 3153–3181.

Pardo-Pascual, J.E., Almonacid-Caballer, J., Ruiz, L.A., Palomar-Vázquez, J., 2012. Automatic extraction of shorelines from Landsat TM and ETM+ multi-temporal images with subpixel precision. Remote Sens. Environ. 123, 1–11. https://doi.org/10.1016/j.rse.2012.02.024.

Parrish, C.E., 2012. In: Yang, X., Li, J. (Eds.), Chapter 6: Shoreline Mapping in Advances in Mapping from Remote Sensor Imagery: Techniques and Applications. CRC Press, Taylor and Francis Group, Boca Raton, Florida, pp. 145–168.

Parrish, C.E., Sault, M., White, S.A., Sellars, J., 2005. Empirical analysis of aerial camera filters for shoreline mapping. In: Proceedings of the American Society for Photogrammetry and Remote Sensing Annual Conference, Baltimore, Maryland. pp. 1–11.

Pianca, C., Holman, R., Siegle, E., 2015. Shoreline variability from days to decades: results of long-term video imaging. J. Geophys. Res. Oceans 120 (3), 2159–2178.

Poornima, K.V., Chinthaparthi, S., 2014. Detection and future prediction of coastal changes in Chennai using remote sensing and GIS techniques. Int. J. Innov. Res. Sci. Eng. Technol. 3 (2), 9456–9462.

Post, J.C., Lundin, C.G., 1996. Guidelines for Integrated Coastal Zone Management.

Rawat, J.S., Kumar, M., 2015. Monitoring land use/cover change using remote sensing and GIS techniques: a case study of Hawalbagh block, district Almora, Uttarakhand, India. Egypt. J. Remote Sens. Space Sci. 18 (1), 77–84. https://doi.org/10.1016/j.ejrs.2015.02.002.

Ruggiero, P., Kaminsky, G.M., Gelfenbaum, G., Voigt, B., 2005. Seasonal to interannual morphodynamics along a high-energy dissipative littoral cell. J. Coast. Res. 553–578.

Sadr, K., Rodier, X., 2012. Google Earth, GIS and stone-walled structures in southern Gauteng, South Africa. J. Archaeol. Sci. 39 (4), 1034–1042.

Sagar, S., Phillips, C., Bala, B., Roberts, D., Lymburner, L., 2018. Generating continental scale pixel-based surface reflectance composites in coastal regions with the use of a multi-resolution tidal model. Remote Sens. 10 (3), 480.

Salghuna, N., Bharathvaj, S.A., 2015. Shoreline change analysis for northern part of the Coromandel Coast. Aquat. Procedia 4, 317–324.

Santos, N.D., Gonçalves, G., 2014. Remote sensing applications based on satellite open data (Landsat 8 and Sentinel-2). In: Conferencia National de Geodecisao Barreiro, May.

de Schipper, M.A., de Vries, S., Ruessink, G., de Zeeuw, R.C., Rutten, J., van Gelder-Maas, C., Stive, M.J., 2016. Initial spreading of a mega feeder nourishment: observations of the sand engine pilot project. Coast. Eng. 111, 23–38.

Shin, B., Kim, K., 2015. Estimation of shoreline change using high resolution images. Procedia Engineering 116, 994–1001. https://doi.org/10.1016/j.proeng.2015.08.391.

Siakor, S.K.A., 2014. Illegal logging persists in Liberia, news paper. Pambazuka Newsavailable on http://www.pambazuka.org/printpdf/89095, (November, 2016).

Smith Jr, J.T., 1981. A History of Flying and Photography in the Photogrammetry Division of the National Ocean Survey, 1919–79. vol. 486, U.S. Department of Commerce, National Oceanic and Atmospheric Administration, National Ocean Service, Silver Spring, Maryland.

Song, C., Woodcock, C.E., Seto, K.C., Lenney, M.P., Macomber, S.A., 2001. Classification and change detection using Landsat TM data: when and how to correct atmospheric effects?. Remote Sens. Environ. 75 (2), 230–244.

Stockdon, H.F., Sallenger Jr, A.H., List, J.H., Holman, R.A., 2002. Estimation of shoreline position and change using airborne topographic lidar data. J. Coast. Res. 18 (3), 502–513.

The World Bank, 2016. Liberia IBRD.IDA. Available on http://www.worldbank.org/en/country/liberia, (November, 2016).

Tochamnanvita, T., Muttitanon, W., 2014. Investigation of coastline changes in three provinces of Thailand using remote sensing. ISPRS XL-8, 1079–1083. https://doi.org/10.5194/isprsarchives-XL-8-1079-2014.

Topouzelis, K., Spondylidis, S.C., Papakonstantinou, A., Soulakellis, N., 2016, August. The use of Sentinel-2 imagery for seagrass mapping: Kalloni Gulf (Lesvos Island, Greece) case study. In: Fourth International Conference on Remote Sensing and Geoinformation of the Environment (RSCy2016). vol. 9688, International Society for Optics and Photonics, p. 96881F.

Turner, I.L., Harley, M.D., Short, A.D., Simmons, J.A., Bracs, M.A., Phillips, M.S., Splinter, K.D., 2016. A multi-decade dataset of monthly beach profile surveys and inshore wave forcing at Narrabeen, Australia. Sci. Data 3, 160024.

UN DESA, 2015. World Population Prospects 2015. Available on https://esa.un.org/unpd/wpp/, (October, 2016).

UNDP, 2006. First State of the Environment Report for Liberia - 2006. In: https://www.thegef.org/sites/default/files/ncsa-documents/State_of_the_environment_report_final.pdf, (August, 2018).

UNDP, 2015. The Republic of Liberia: Enhancing the Resilience of Vulnerable Coastal Areas to Climate Change Risks. Available on http://adaptation-undp.org/sites/default/files/downloads/brief_3975_liberia.pdf, (September, 2016).

UNEP, 2004. Desk study on the environment in Liberia. United Nations Environment Programme, Geneva, In: https://postconflict.unep.ch/publications/Liberia_DS.pdf, (August, 2018).

USAID, 2012. Climate Change Adaptation in Liberia. available on https://www.climatelinks.org/sites/default/files/asset/document/liberia_adaptation_fact_sheet_jan2012.pdf, (October, 2016).

USGS, 2015. Landsat Data. USGS, United States.

Veloso-Gomes, A., Barroco, A.R., Pereira, C.S., Reis, H., Calado, J.G., Ferreira, M.D.C., Freitas, Biscoito, M., 2008. Basis for a national strategy for integrated coastal zone management—in Portugal. J. Coast. Conservat. 12, 3–9.

Werrell, C., Femia, F., 2014. Liberia's rising waters. In: Climate and Security, available on https://climateandsecurity.org/2014/08/19/liberias-rising-waters/, (November, 2016).

Westoby, M.J., Brasington, J., Glasser, N.F., Hambrey, M.J., Reynolds, J.M., 2012. 'Structure-from-motion' photogrammetry: a low-cost, effective tool for geoscience applications. Geomorphology 179, 300–314.

White, K., El Asmar, H.M., 1999. Monitoring changing position of coastlines using thematic mapper imagery, an example from the Nile Delta. Geomorphology 29 (1–2), 93–105.

White, S.A., Parrish, C.E., Calder, B.R., Pe'eri, S., Rzhanov, Y., 2011. Lidar-derived national shoreline: empirical and stochastic uncertainty analyses. J. Coast. Res. Spec. Issue 62, 62–74.

Wiles, D., 2005. Coastal zone vulnerability and adaptation to climate change in Liberia. In: Paper Presented at the Training Workshop on Adaptation and Vulnerability to Climate Change, Maputo, Mozambique.

Williams, W.C.L., 2016. Liberia's poor and the rising sea. available on Inter Press Servicehttp://www.ipsnews.net/2014/06/liberias-poor-and-the-rising-sea/, (November, 2016).

Yao, F., Parrish, C.E., Pe'eri, S., Calder, B.R., Rzhanov, Y., 2015. Modeling uncertainty in photogrammetry-derived national shoreline. Mar. Geod. 28, 128–145.

Yu, K., Hu, C., Muller-Karger, F.E., Lu, D., Soto, I., 2011. Shoreline changes in west-central Florida between 1987 and 2008 from Landsat observations. Int. J. Remote Sens. 32 (23), 8299–8313. https://doi.org/10.1080/01431161.2010.535045.

Zhang, Y., Li, X., Zhang, J., Song, D., 2013. A study on coastline extraction and its trend based on remote sensing image data mining. Abstr. Appl. Anal. 2013, 1–6. https://doi.org/10.1155/2013/693194.